

*Supporting information*

A novel near-infrared ytterbium complex $[\text{Yb}(\text{DPPDA})_2](\text{DIPEA})$ with $\varphi = 0.46\%$ and $\tau_{\text{obs}} = 105 \mu\text{s}$

Guozhu Ren ^{1,2}, Danyang Zhang ^{1,2}, Hao Wang ³, Xiaofang Li ^{1,2}, Ruiping Deng ¹, Shihong Zhou ¹, Long Tian ¹, Liang Zhou ^{1,2,*}

¹ State Key Laboratory of Rare Earth Resource Utilization, Changchun Institute of Applied Chemistry, Chinese Academy of Sciences, Changchun 130022, China; rgz666@ciac.ac.cn (G.R.); dyzhang26@ciac.ac.cn (D.Z.); xflizkd@ciac.ac.cn (X.L.); dengrp@ciac.ac.cn (R.D.); shzhou@ciac.ac.cn (S.Z.); tianlong@ciac.ac.cn (L.T.)

² School of Applied Chemistry and Engineering, University of Science and Technology of China, Hefei 230027, China

³ School of Materials Science and Engineering, Jilin Jianzhu University, Changchun 130118, China; 13341427152@163.com

* Correspondence: zhoul@ciac.ac.cn; Tel.: +86-431-85262855; Fax: +86-431-85698041

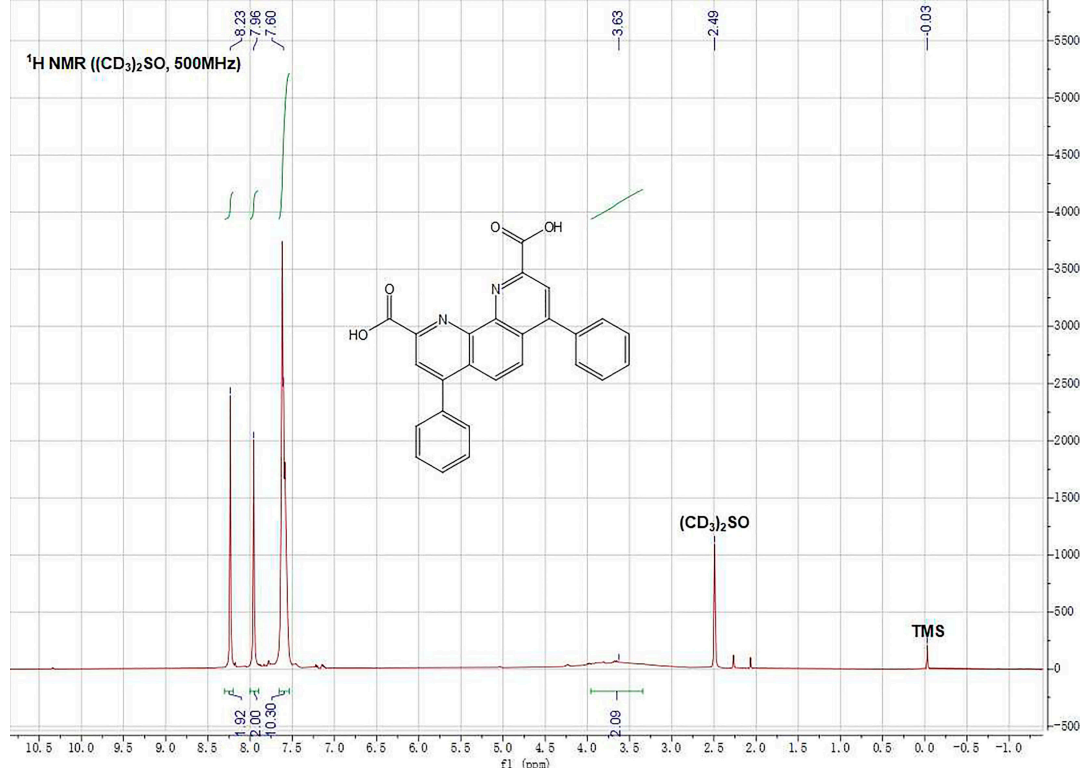


Figure S1. ¹H NMR spectrum of 4,7-diphenyl-1,10-phenanthroline-2,9-dicarboxylic acid (DPPDA).

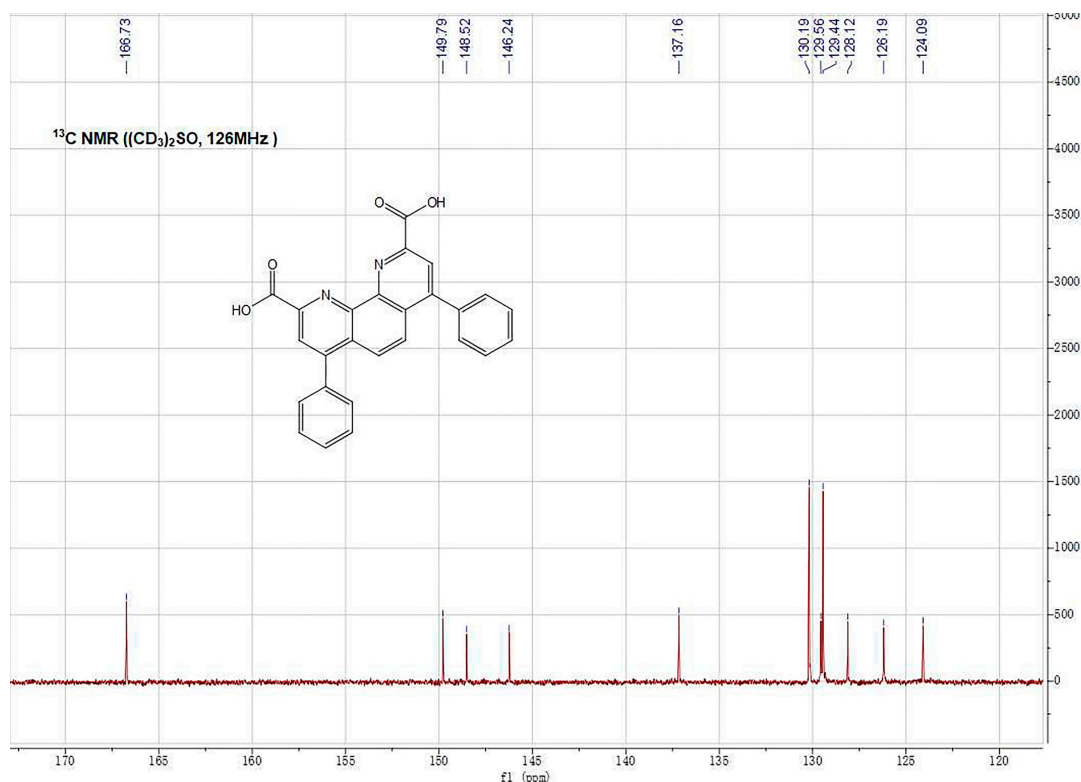


Figure S2. ^{13}C NMR spectrum of DPPDA.

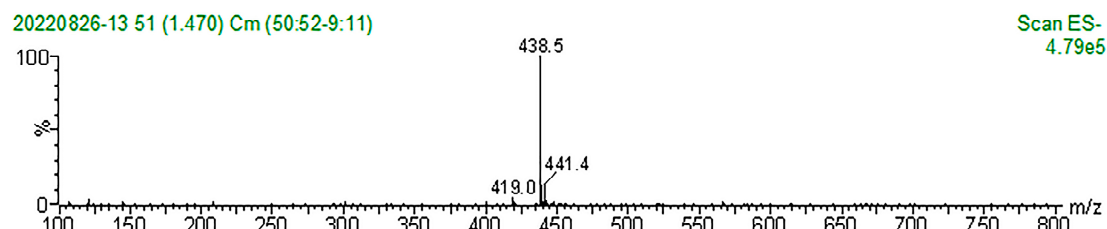


Figure S3. ESI-MS spectrum of DPPDA (CH₃CH₂OH negative mode).

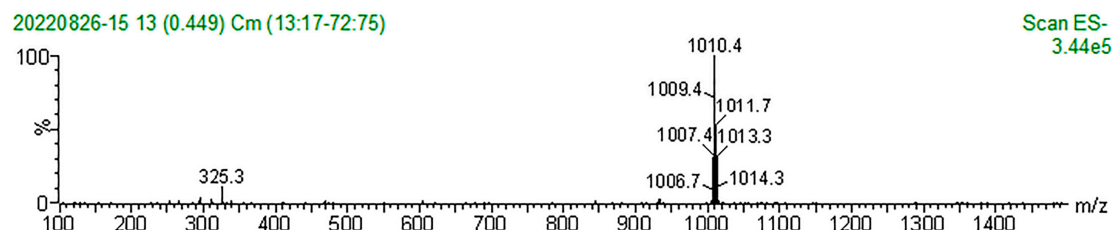
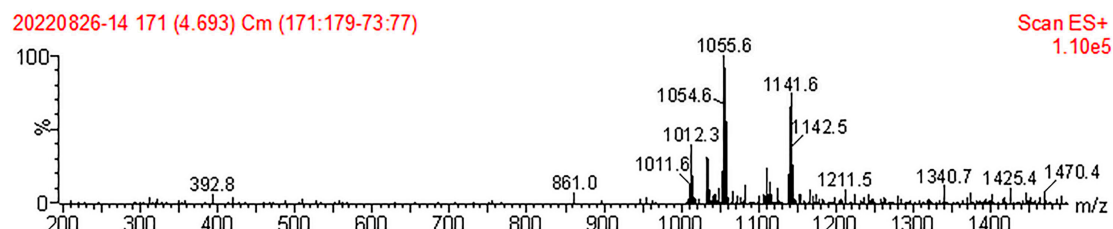
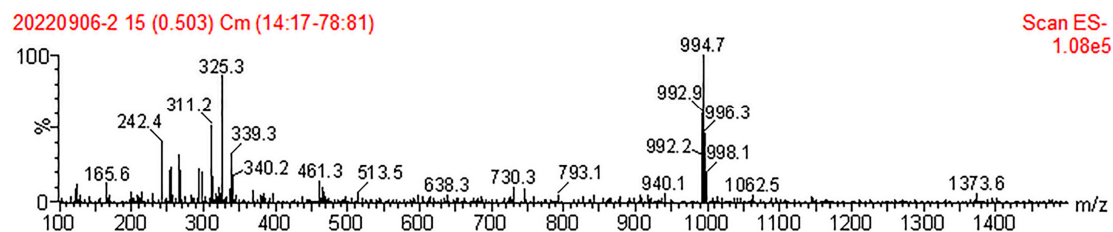
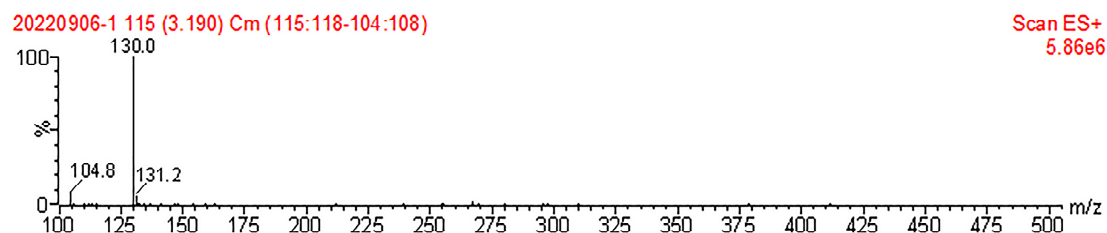
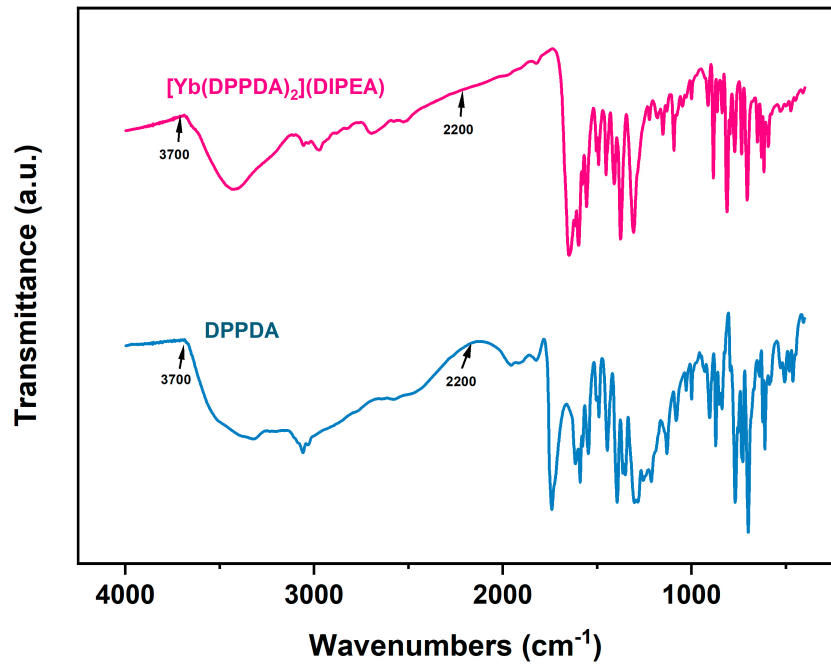


Figure S4. ESI-MS spectrum of [Yb(DPPDA)₂](DIPEA) (CHCl₃ negative mode).



**Figure S5.** ESI-MS spectrum of $[Yb(DPPDA)_2](DIPEA)$ ($CHCl_3$ positive mode).**Figure S6.** ESI-MS spectrum of $[Gd(DPPDA)_2](DIPEA)$ ($CHCl_3$ negative mode).**Figure S7.** ESI-MS spectrum of $[Gd(DPPDA)_2](DIPEA)$ ($CHCl_3$ positive mode).**Figure S8.** FT-IR spectra of DPPDA and $[Yb(DPPDA)_2](DIPEA)$ in the range of $4000\sim400\text{ cm}^{-1}$.

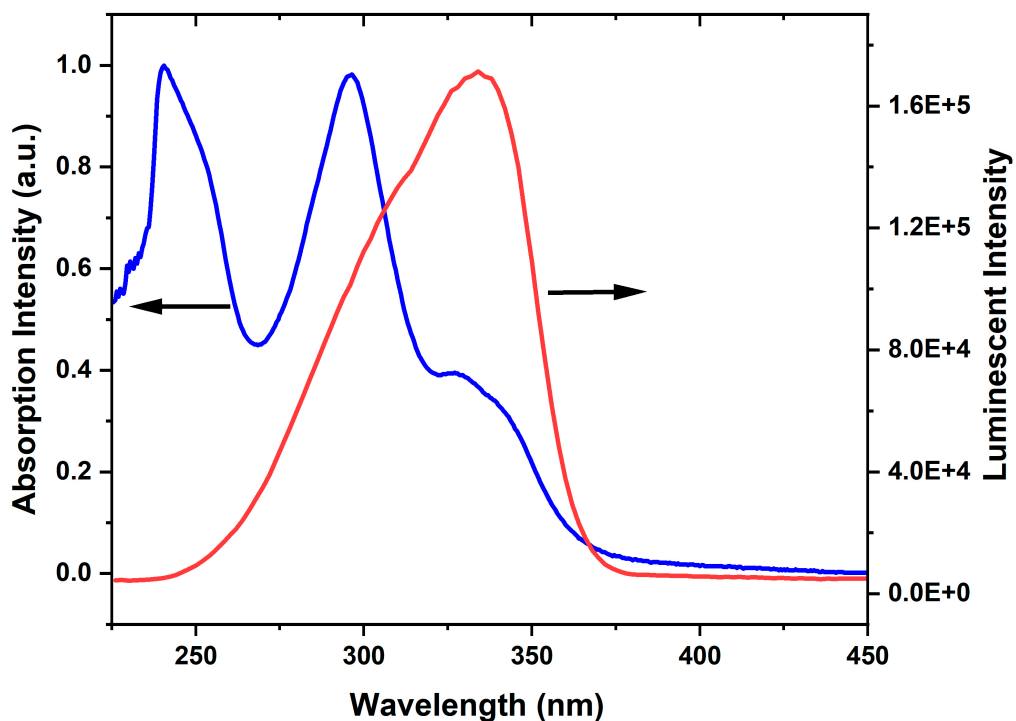
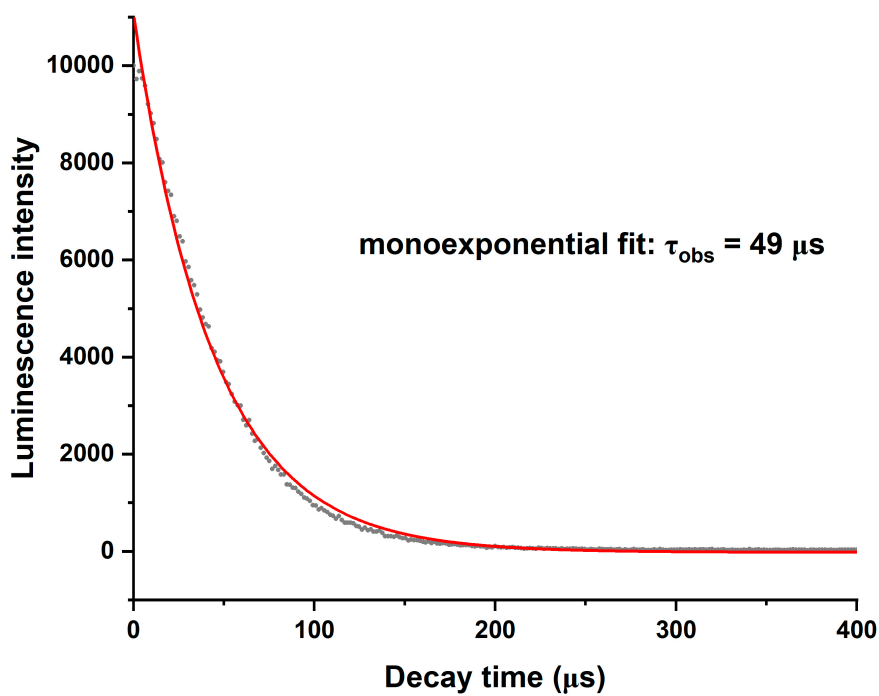


Figure S9. UV-Vis absorption spectrum and excitation spectrum ($\lambda_{\text{monitor}} = 1011 \text{ nm}$) of $[\text{Yb}(\text{DPPDA})_2](\text{DIPEA})$ at room temperature.



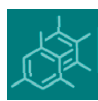


Figure S10. Luminescence decay profile of the transition $^2\text{F}_{5/2} \rightarrow ^2\text{F}_{7/2}$ ($\lambda_{\text{em}} = 1011$ nm) in $[\text{Yb}(\text{DPPDA})_2](\text{DIPEA})$ (CHCl_3 , $\lambda_{\text{ex}} = 335$ nm, monoexponential fit in red) at room temperature.

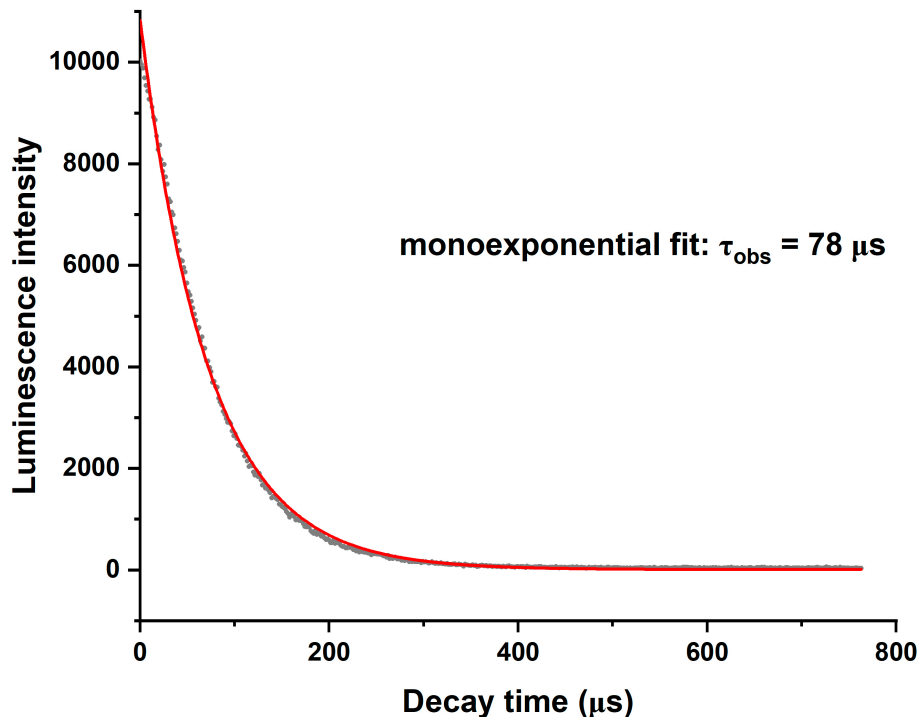


Figure S11. Luminescence decay profile of the transition $^2\text{F}_{5/2} \rightarrow ^2\text{F}_{7/2}$ ($\lambda_{\text{em}} = 1011$ nm) in $[\text{Yb}(\text{DPPDA})_2](\text{DIPEA})$ (CDCl_3 , $\lambda_{\text{ex}} = 335$ nm, monoexponential fit in red) at room temperature.

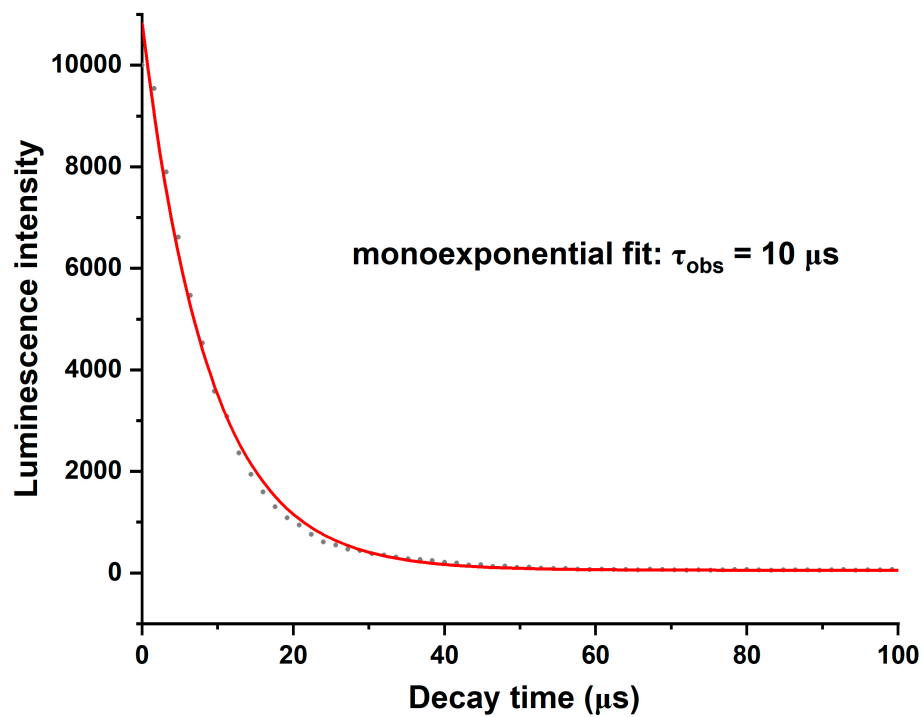
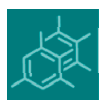


Figure S12. Luminescence decay profile of the transition $^2\text{F}_{5/2} \rightarrow ^2\text{F}_{7/2}$ ($\lambda_{\text{em}} = 1011 \text{ nm}$) in $[\text{Yb}(\text{DPPDA})_2](\text{DIPEA})$ (CH_3OH , $\lambda_{\text{ex}} = 335 \text{ nm}$, monoexponential fit in red) at room temperature.

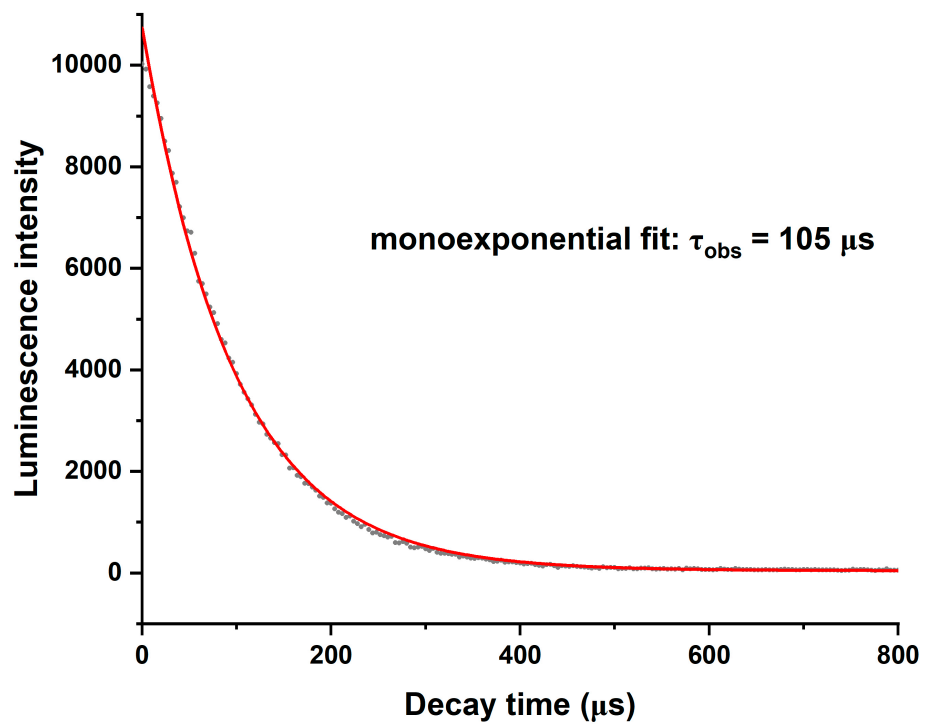
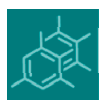


Figure S13. Luminescence decay profile of the transition ${}^2\text{F}_{5/2} \rightarrow {}^2\text{F}_{7/2}$ ($\lambda_{\text{em}} = 1011 \text{ nm}$) in $[\text{Yb(DPPDA)}_2](\text{DIPEA})$ (CD_3OD , $\lambda_{\text{ex}} = 335 \text{ nm}$, monoexponential fit in red) at room temperature.

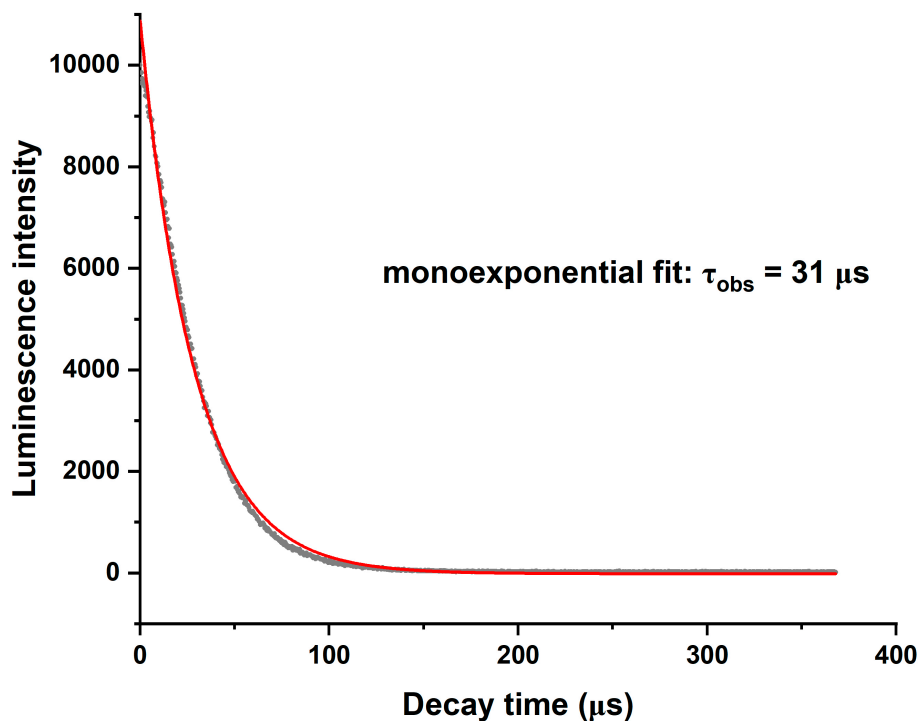


Figure S14. Luminescence decay profile of the transition $^2\text{F}_{5/2} \rightarrow ^2\text{F}_{7/2}$ ($\lambda_{\text{em}} = 1011 \text{ nm}$) in $[\text{Yb(DPPDA)}_2](\text{DIPEA})$ (solid, $\lambda_{\text{ex}} = 335 \text{ nm}$, monoexponential fit in red) at room temperature.

Solvent ¹	S_R^2	S_s^3	E_s^4	QYs ⁵ (%)
solid	9.26E+08	8.10E+07	1.31E+05	0.06
CH_3OH	1.04E+09	3.18E+07	3.98E+04	0.02
CD_3OD	4.95E+08	1.56E+07	5.58E+05	0.46
CHCl_3	4.89E+08	1.66E+07	2.69E+05	0.22
CDCl_3	4.31E+08	2.63E+07	3.87E+05	0.37

¹Measuring condition: $\lambda_{\text{ex}} = 335 \text{ nm}$, $\lambda_{\text{em}} = 1011 \text{ nm}$, $1 \times 10^{-4} \text{ mol/L}$, 298 K. ² S_R = Integrated scattering intensity of reference cell. ³ S_s = Integrated scattering intensity of sample. ⁴ E_s = Integrated emission intensity of sample. ⁵The calculation formula of QYs is: $(\text{F} * \text{E}_s) / (\text{S}_R * \text{S}_s)$, F is correction factor aimed to eliminate the influence of different sensitivity between UV-Vis detector (180 nm—900 nm) and NIR detector (600 nm—1700 nm). By measuring and contrasting detected light intensity of the spectral overlapping region (700 nm—800 nm) of two detectors, F is calculated to be 3.91.

Table S1. The measuring data of absolute quantum yields of $[\text{Yb(DPPDA)}_2](\text{DIPEA})$ in different solutions and solid state at room temperature.

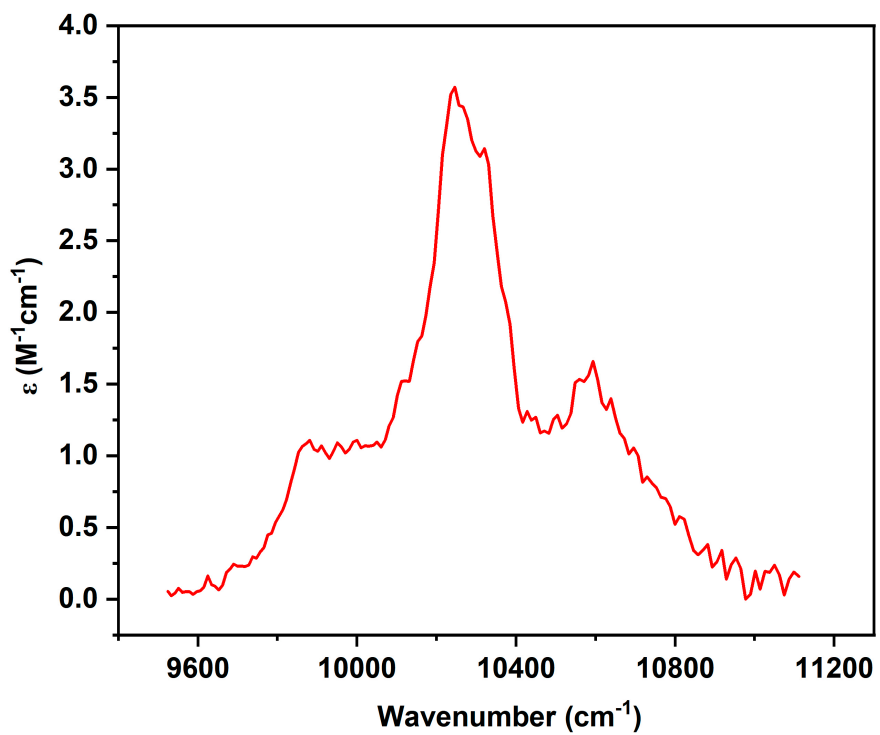
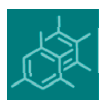


Figure S15. NIR absorption spectrum of the f-f transition $^2\text{F}_{7/2} \rightarrow ^2\text{F}_{5/2}$ in $[\text{Yb}(\text{DPPDA})_2](\text{DIPEA})$ (in 4×10^{-4} mol/L CD_3OD solution).

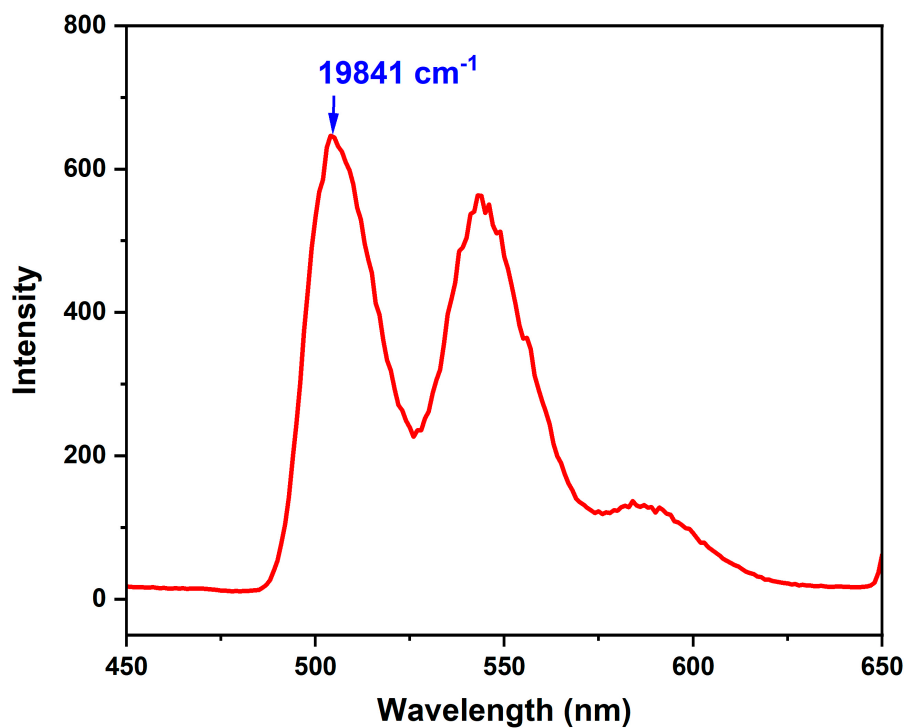


Figure S16. Low temperature fluorescence spectrum of $[\text{Gd}(\text{DPPDA})_2](\text{DIPEA})$ ($\lambda_{\text{ex}} = 335 \text{ nm}$, in $1 \times 10^{-4} \text{ mol/L CHCl}_3$ solution).

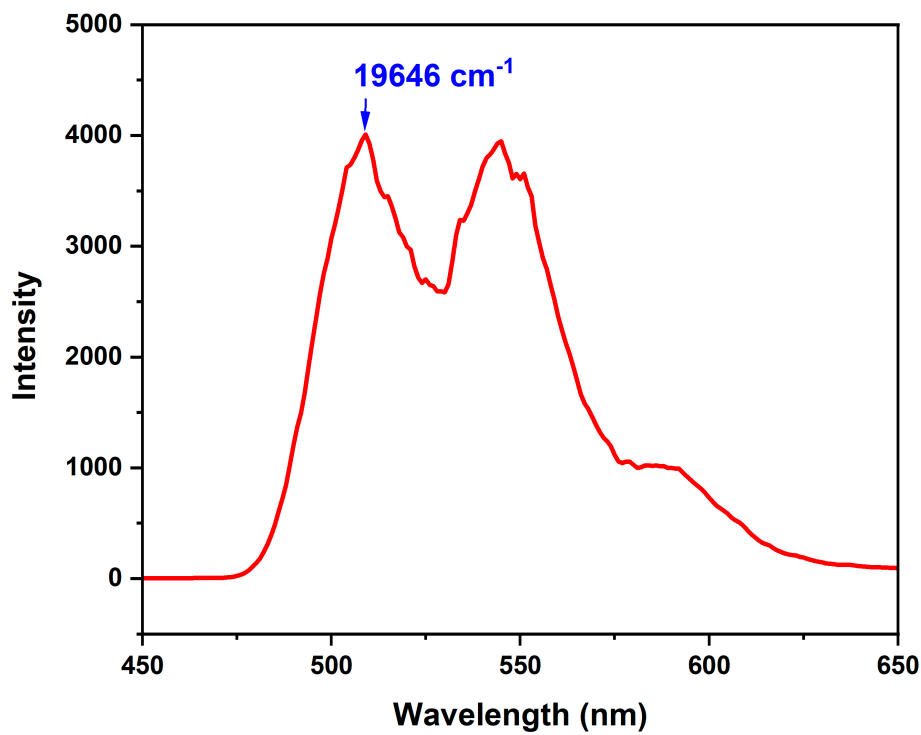


Figure S17. Low temperature phosphorescence spectrum of $[\text{Gd}(\text{DPPDA})_2](\text{DIPEA})$ ($\lambda_{\text{ex}} = 335 \text{ nm}$, in $1 \times 10^{-4} \text{ mol/L CHCl}_3$ solution).

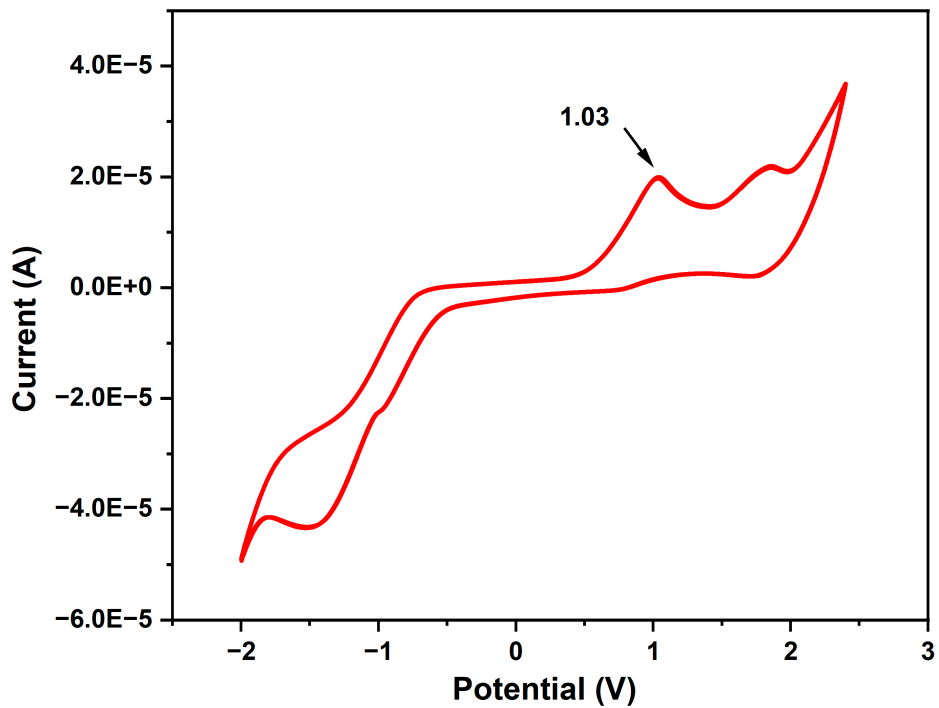


Figure S18. Cyclic voltammogram of $\text{DPPDA}(\text{DIPEA})_2$ (with Ag/AgCl reference electrode in $1 \times 10^{-3} \text{ mol/L CHCl}_3$ solution).

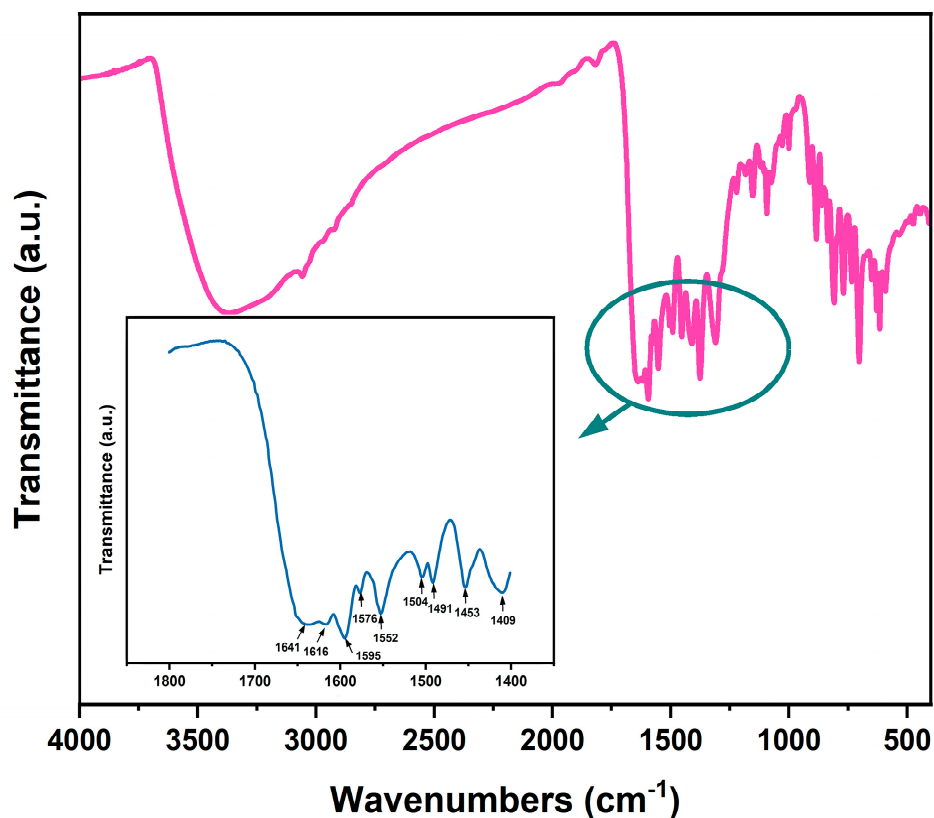


Figure S19. FT-IR spectrum of $[Gd(DPPDA)_2](DIPEA)$ in the range of 4000~400 cm^{-1} (The illustration is enlarged FT-IR spectrum in the range of 1800~1400 cm^{-1}).